NUCLEAR SCIENCE AND TECHNIQUES **26**, S10310 (2015)

The chlorination of La_2O_3 by $MgCl_2$ in the LiCl-NaCl melts*

WANG Ying-Cai (王英财),[1] LI Mei (李梅),[1] HAN Wei (韩伟),[1,†] LIU Yao-Chen (刘垚臣),[1]
LIU Bin (刘斌),[1] YAN Yong-De (颜永得),[1] and ZHANG Mi-Lin (张密林)[1]

[1]*Key Laboratory of Superlight Materials and Surface Technology, Ministry of Education, College of Materials Science and Chemical Engineering, Harbin Engineering University, Harbin 150001, China*

(Received May 9, 2014; accepted in revised form October 23, 2014; published online December 20, 2014)

The chlorination of rare earth oxides by $MgCl_2$ was investigated in the molten chlorides. To reduce the solvent salt volatility, the LiCl-NaCl mixture was selected as a solvent by comparing the mass loss of the LiCl-NaCl with LiCl-KCl melts after the addition of $MgCl_2$ in the temperature range of 873 K to 1073 K. The dissolution behavior of La_2O_3 was investigated in the LiCl-NaCl-$MgCl_2$ melts by XRD measurements and ICP-AES analysis of the melts, which indicated that La_2O_3 was chlorinated by $MgCl_2$ to produce $LaCl_3$. The reduction peak of La(III) in the LiCl-NaCl-$MgCl_2$-La_2O_3 melts was observed from cyclic voltammogram and square wave voltammogram. The Mg-La alloy obtained by galvanostatic electrolysis in the LiCl-NaCl-$MgCl_2$-La_2O_3 melts was characterized by XRD and SEM-EDS, indicating that the Mg-La alloy consisted of Mg and La_2Mg_{17} phases.

Keywords: LiCl-NaCl-$MgCl_2$ melts, Chlorination, La_2O_3, Mg-La alloy

DOI: 10.13538/j.1001-8042/nst.26.S10310

I. INTRODUCTION

Molten salts, particularly molten chlorides, are well known as good reaction media for performing selective solubilization or precipitation in chemical reactions, and have already been proposed as a promising route for the treatment of raw materials [1]. Pyrochemical separation processes in molten media have more recently been proposed as a promising option in the nuclear fuel cycle for the future [2, 3]. Since rare earth chloride is extremely sensitive to O_2 and H_2O, rare earth oxides employed as the raw material of rare earth elements, which greatly simplified the production process and reduced the production cost. But rare earth oxides are usually insoluble in molten chlorides [4]. Thus the direct chlorination of rare earth oxides in the melts was studied in chlorides melts. Sakamura *et al*. [5] reported that rare earth oxides could be chlorinated by $ZrCl_4$ in LiCl-KCl eutectic melts. Our previous work showed that $AlCl_3$ could chloride the Pr_6O_{11} [6] and Eu_2O_3 [7] in KCl-LiCl melts.

But $AlCl_3$ and $ZrCl_4$ have a very low melting point and can be sublimed easily [8]. In order to avoid the sublime of chlorination reagent, $MgCl_2$ was chosen to chloride rare earth oxides. Since the melting point and boiling point of magnesium chloride are higher than those of $AlCl_3$ and $ZrCl_4$, to prevent from solvent salt volatility, appropriate solvent was selected by measuring the mass loss of LiCl-NaCl and LiCl-KCl melts by adding $MgCl_2$ at high temperature. And then the chlorination of La_2O_3 by $MgCl_2$ in the selected LiCl-NaCl melts was explored by a series of techniques. To further confirm the chlorination of La_2O_3 by $MgCl_2$, galvanostatic electrolysis was carried out to produce Mg-La alloy characterized by XRD and SEM-EDS.

II. EXPERIMENTAL

A. Preparation and purification of melts

The mixture of LiCl-NaCl (60 : 30 wt.%, analytical grade) and LiCl-KCl(40 : 50 wt.%, analytical grade) was first dried under vacuum for more than 24 h at 573 K to remove excess water, and then melted in an alumina crucible placed in a quartz cell putted in an electric furnace. The temperature of melts was measured with a nickel chromium-nickel aluminium thermocouple sheathed with an alumina tube. Magnesium and Lanthanum ions were introduced into the bath in the form of dehydrated $MgCl_2$ (99.9%, analytical grade) and La_2O_3 powder (99.9%, analytical grade). The concentration of La_2O_3 in the LiCl-NaCl-$MgCl_2$ melts was analyzed by inductively coupled plasma atomic emission spectrometer (ICP-AES, Thermo Elemental, IRIS Intrepid II XSP). All experiments were performed in an inert argon atmosphere (99.999%, high pure liquid Argon) to prevent from moisture.

B. Electrochemical apparatus and electrodes

All electrochemical measurements were carried out using an Auto lab electrochemical workstation (Metrohm Co., Ltd.) with the Nova 1.10 software package. A silver wire (d = 1 mm) dipped into a solution of AgCl (0.070 mol/kg) in LiCl-NaCl melts contained in a pyrex tube was used as a reference electrode. All potentials were referred to Ag/AgCl couple. A spectrally pure graphite rod (d = 6 mm) served as

* Supported by Key Laboratory of Superlight Materials and Surface Technology, Ministry of Education, the National Natural Science foundation of China (Nos. 21271054 and 21173060), the Major Research plan of the National Natural Science Foundation of China (Nos. 91326113 and 91226201) and the Fundamental Research funds for the Central Universities (No. HEUCF201403001)

† Corresponding author, weihan@hrbeu.edu.cn

the counter electrode. The working electrodes were tungsten (W) wires (d = 0.9 mm, 99.99% purity), which were polished thoroughly using SiC paper, then cleaned ultrasonically with ethanol (99.8% purity) in an ultrasonic bath prior to use.

C. Preparation and characterization of samples

All samples were cleaned in ethanol in an ultrasonic bath to remove salts and stored in a glove box for analysis. These deposits were analyzed by X-ray diffraction (XRD, X'Pert Pro; Philips Co., Ltd.) using Cu K_α radiation at 40 kV and 40 mA. The microstructure and microzone chemical analyses were also carried out using scanning electron microscope with Energy dispersive spectroscopy (SEM-EDS, JSM-6480A; JEOL Co., Ltd.).

III. RESULTS AND DISCUSSION

A. The choice of new chloride system

There are numerous selection criteria for choosing the molten salt system, such as salt stability, salt volatility, solubility of metallic species and so on. It is important to select salt mixtures as solvent medium in order to reduce the salt loss and increase the solubility of RE_2O_3 in the molten salt. The details are as follow.

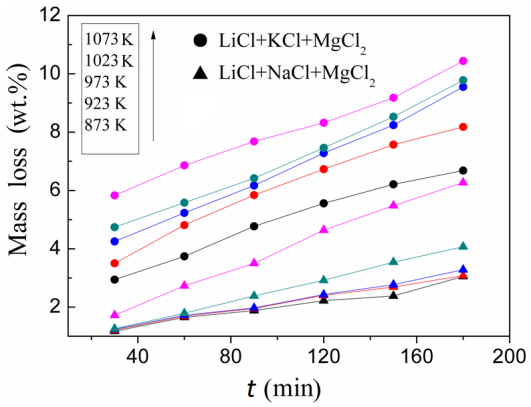

Fig. 1. (Color online) The mass loss of the two molten melts at different temperature.

The mixture of an anhydrous LiCl-NaCl-$MgCl_2$ (6.0 : 3.0 : 1.5 wt.%) and LiCl-KCl-$MgCl_2$ (4.0 : 5.0 : 1.5 wt.%) powder in a corundum crucible and heated to a specified temperature in electric furnace under argon atmosphere. The mass loss of the two systems of LiCl-NaCl-$MgCl_2$ and LiCl-KCl-$MgCl_2$ were measured in every 30 min using an electronic balance in the temperature range from 873 K to 1073 K. The comparison of mass loss in these two different systems was shown in Fig. 1. The results showed that the mass loss in the LiCl-KCl-$MgCl_2$ molten salts was much larger than that in the LiCl-NaCl-$MgCl_2$, thus proving that LiCl-NaCl-$MgCl_2$ melts are more stable than LiCl-KCl-$MgCl_2$ melts in the experimental temperature range. According to the experimental results, a new salt system, LiCl-NaCl melts, was selected as a solvent.

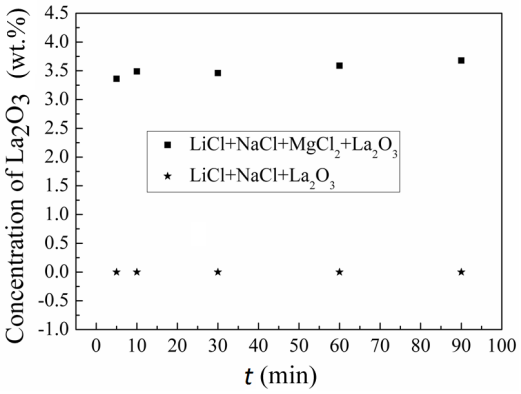

Fig. 2. The concentration of the La_2O_3 in the LiCl-NaCl and LiCl-NaCl-$MgCl_2$ melts at 873 K.

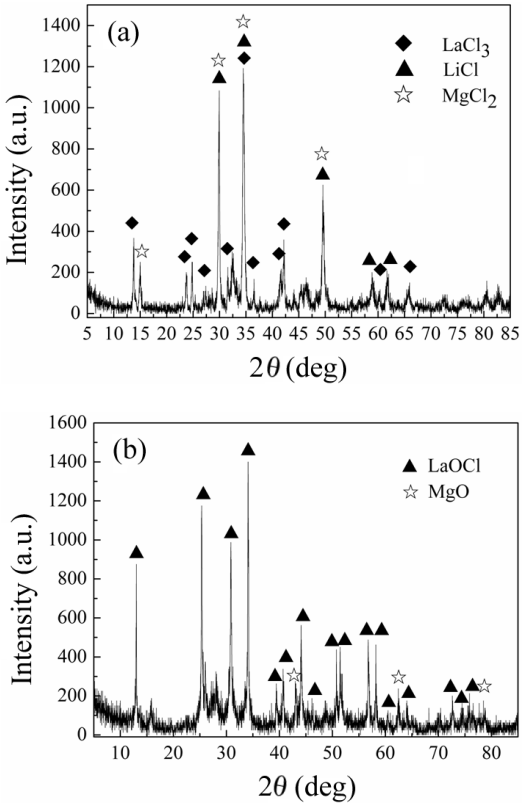

Fig. 3. XRD patterns of (a) supernatant melts in LiCl-NaCl-$MgCl_2$-La_2O_3 melts and (b) non-dissolved residues in LiCl-NaCl-$MgCl_2$-La_2O_3 melts.

B. Chlorination of La_2O_3 by $MgCl_2$ in the LiCl-NaCl melts

The concentration of La_2O_3, i.e. the concentration of La(III) ions in LiCl-NaCl melts was determined by ICP. Anhydrous LiCl-NaCl-La_2O_3 (6.0 : 3.0 : 0.5 wt.%) and LiCl-NaCl-$MgCl_2$-La_2O_3 (6.0 : 3.0 : 1.5 : 0.5 wt.%) powder in a corundum crucible were heated to 873 K in electric furnace under argon atmosphere and stirred to dissolve fully. Supernatant fluid of molten salts was taken out and analyzed by ICP-AES and XRD. Fig. 2 shows the results of ICP-AES analysis of supernatant fluid with the LiCl-NaCl-La_2O_3 and LiCl-NaCl-$MgCl_2$-La_2O_3 melts. The results show that La_2O_3 can hardly dissolve in the LiCl-NaCl-La_2O_3 melts, but the concentration of La_2O_3 in the LiCl-NaCl-$MgCl_2$-La_2O_3 melts can reach 3.68 wt.%. Evidently, the existence of $MgCl_2$ can accelerate the solubilization of La_2O_3.

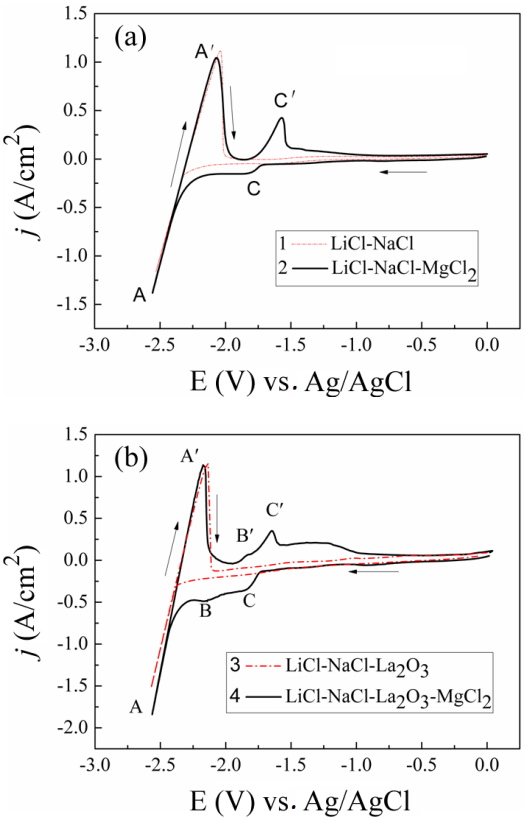

Fig. 4. (Color online) The typical cyclic voltammograms on a W electrode (S = 0.322 cm^2) at 873 K from the (a) LiCl -NaCl melts before (curve 1) and after (curve 2) the addition of 1.0 wt.% $MgCl_2$; (b) LiCl-NaCl-La_2O_3 (2 wt.%) melts before (curve 3) and after (curve 4) the addition of 1.0 wt.% $MgCl_2$; scan rate: 0.1 V/s.

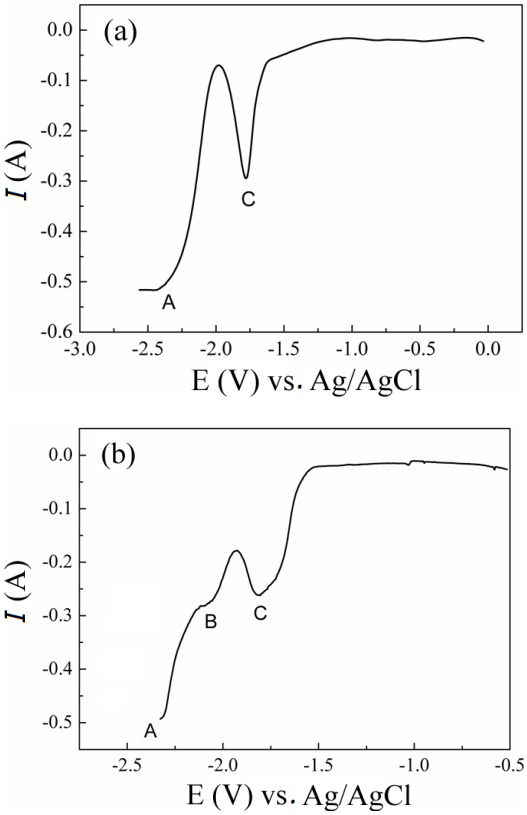

Fig. 5. Square wave voltammograms from LiCl-NaCl-La_2O_3 melts before (a) and after (b) the addition of $MgCl_2$ on a W electrode (S=0.322 cm^2) at 873 K. Pulse height: 25 mV; potential step: 1 mV; frequency: 25 Hz.

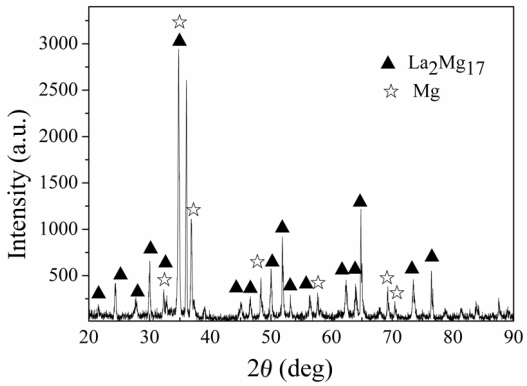

Fig. 6. XRD patterns of Mg-La alloy obtained by galvanostatic electrolysis at 1 A in the LiCl-NaCl-$MgCl_2$ (10 wt.%)-La_2O_3(2 wt.%) melts at 873 K for 3 h.

Figure 3(a) shows the XRD pattern of the dissolved supernatant salt of the LiCl-NaCl-$MgCl_2$ melts. It can be seen that the $LaCl_3$ exists in the LiCl-NaCl-$MgCl_2$ melts. Since the rare earth oxides and oxychlorides are insoluble in KCl-LiCl eutectic melts [9], MgO and La_2O_3 remain solid particles and precipitates in LiCl-NaCl melts. The melts cooled were washed with water in order to remove the soluble salts, and then filter to obtain insoluble substance. The insoluble substance was characterized by XRD shown in Fig. 3(b). The result indicated that the insoluble substance contained LaOCl and MgO. According to Bentouhami [10], LaOCl maybe forms due to the hydrolysis of $LaCl_3$ during the melts being washed with water. From the results mentioned above, we suggest that La_2O_3 is chlorinated by $MgCl_2$ to form $LaCl_3$.

$$3MgCl_2 + La_2O_3 \rightarrow 2LaCl_3 + 3MgO. \quad (1)$$

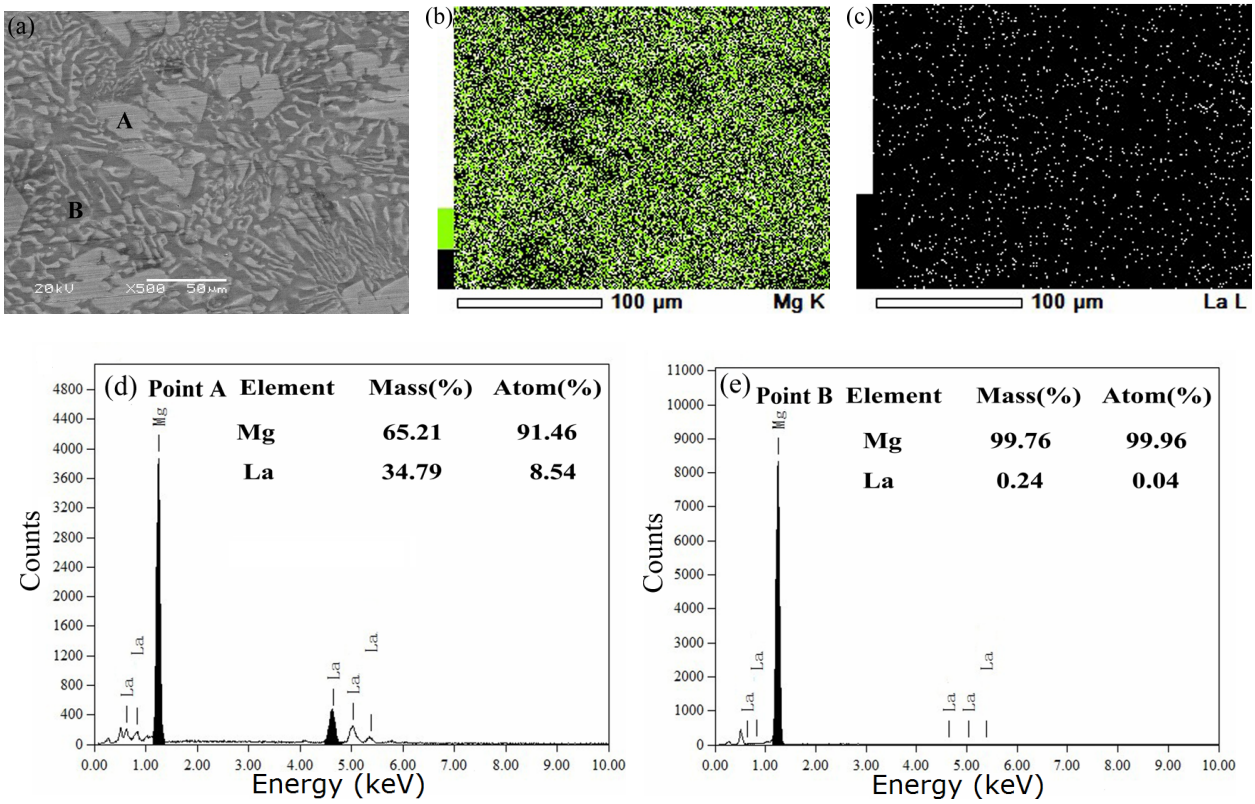

Fig. 7. (Color online) SEM image and EDS mapping analysis of Mg-La alloy obtained in the LiCl-NaCl-$MgCl_2$ (10 wt.%)-La_2O_3(2 wt.%) melts at 873 K; a: SEM image; b and c: EDS mapping analysis of Mg and La; d and e: the EDS analysis of points labeled A and B in the Fig. 7(a).

Figure 4(a) shows the typical cyclic voltammograms (CVs) in LiCl-NaCl melts before and after the addition of 1.0 wt.% $MgCl_2$ on W electrodes at 873 K. In curve 1, the cathodic signal A observed in the absence of $MgCl_2$ in LiCl-NaCl melts is ascribed to the deposition of Li(I) ions, since no alloy or intermetallic compounds exist in the phase diagram of the W-Li binary system [11] at 873 K. In the reverse scanning direction, an anodic peak A' is corresponding to the dissolution of Li metal. After adding 1.0 wt.% $MgCl_2$, except for the peaks A/A', peaks C/C' are associated with the reduction and reoxidation of Mg metal. The results are consistence with our previous work [12]. Fig. 4(b) shows the CVs in LiCl-NaCl-La_2O_3 (2 wt.%) melts before and after the addition of 1.0 wt.% $MgCl_2$ on W electrodes at 873 K. The shape of curve 3 is the same as the curve 1 in Fig. 3(a), which means that the reduction peak of La (III) ions does not exist, i.e. La_2O_3 powder is nearly insoluble in the LiCl-NaCl-La_2O_3 melts. In curve 4, the CVs shows two new redox couples after the addition of 1.0 wt.% $MgCl_2$ in LiCl-NaCl-La_2O_3 melts. The C/C' peaks are corresponding to the deposition and subsequent oxidation of Mg metal, and the cathodic peak B observed at about −2.07 V is ascribed to the reduction of La(III) ions. The results are in agreement with the ones reported by Masset *et al.* and our previous work [13, 14]. The CVs indicate the existence of La(III) ions in LiCl-NaCl-La_2O_3 melts after the addition of $MgCl_2$.

Figure 5 shows the square wave voltammograms from the LiCl-NaCl-La_2O_3 melts before (a) and after (b) the addition of $MgCl_2$ at a step potential of 1 mV and frequency of 25 Hz. There is only one peak C at −1.80 V, corresponding to the formation of pure Mg in the LiCl-NaCl-La_2O_3 melts (Fig. 5(a)). But the two obvious peaks B and C, observed at −1.80 V and −2.07 V, are attributed to the formation of Mg and La metal in the LiCl-NaCl-La_2O_3 melts after the addition of $MgCl_2$ (Fig. 5(b)). This result indicates that the reduction of La(III)/La(0) is present, in other words, La_2O_3 can be chlorinated by $MgCl_2$ to form La(III) ions.

C. Preparation and characterization of Mg-La alloy

The existence of La(III) ions in the LiCl-NaCl-$MgCl_2$-La_2O_3 melts was explored by electrochemical techniques. To further demonstrate the chlorination effect of $MgCl_2$ on rare earth oxide, the galvanostatic electrolysis was conducted in the LiCl-NaCl-$MgCl_2$(10 wt.%)-La_2O_3(2 wt.%) melts. If we want to obtain a large of mass Mg-La alloy in a relatively short time, we have to perform the electrolysis at a more negative current density. Fig. 6 shows that XRD pattern of Mg-La alloy obtained by galvanostatic electrolysis at 1 A for 3 h. As seen from the XRD pattern, the Mg-La alloy is composed of Mg and La_2Mg_{17}.

To examine the distribution of elements of the Mg and La in the Mg-La alloy, a mapping analysis of the elements was employed. Fig. 7 shows a group of SEM and EDS mapping analysis of the Mg-La alloy obtained from LiCl-NaCl-$MgCl_2$ (10 wt.%)-La_2O_3 (2 wt.%) melts at 873 K. We can find that the La element mainly distributes in the grey zone in the SEM photograph of the alloy. To further investigate the distribution of the element La, a SEM equipped with EDS quantitative analysis was carried out (Figs. 7(d) and 7(e)). The EDS results of the points labeled as A and B taken from grey zone and the dark grey zone indicate that the deposit is composed of elements of Mg and La.

IV. CONCLUSION

According to the determination of the concentration of La(III) in the LiCl-NaCl-$MgCl_2$-La_2O_3 melts and XRD pattern measurements, La_2O_3 can be solubilized by $MgCl_2$ chlorination. A series of electrochemical techniques and the formation of Mg-La alloy obtained by galvanostatic electrolysis further confirm the existence of La(III) in the LiCl-NaCl-$MgCl_2$-La_2O_3 melts. The results indicate that La_2O_3 can be chlorinated by $MgCl_2$: $3MgCl_2 + La_2O_3 \rightarrow 2LaCl_3 + 3MgO$, which may be used for the treatment of the waste nuclear fuel with pyrometallurgy.

[1] Ferry D M, Picard G S, Trémilllon B L. Pulse and ac impedance studies of the electrochemical systems of titanium in LiCl-KCl eutecyic melt at 743K. T I Min Metall A, 1988, **97**: C21–30.

[2] Koyama T, Iizuka M, Tanaka H, *et al*. An experimental study of molten salt electrorefining of uranium using solid iron cathode and liquid cadmium cathode for development of pyrometallurgical reprocessing. J Nucl Sci Technol, 1997, **34**: 384–393.

[3] Inoue T, Sakamura Y, Gaune-Escard M. Molten salts-from fundamentals to applications. NATO science series II, Dordrecht, Kluwer Academic Publishers, 2002: 249–261.

[4] Castrillejo Y, Bermejo M R, Barrado E, *et al*. Cathodic behaviour of europium(III) on glassy carbon, electrochemical formation of Al_4Eu, and oxoacidity reactions in the eutectic LiCl-KCl. J Electroanal Chem, 2007, **545**: 141–157. DOI: 10.1016/j.jelechem.2007.01.018

[5] Sakamura Y, Inoue T, Iwai T, *et al*. Chlorination of UO_2, PuO_2 and rare earth oxides using $ZrCl_4$ in LiCl-KCl eutectic melt. J Nucl Mater, 1997, **340**: 39–51. DOI: 10.1016/j.jnucmat.2004.11.002

[6] Tang H, Yan Y D, Zhang M L, *et al*. $AlCl_3$-aided extraction of praseodymium from Pr6O11 in LiCl-KCl eutectic melts. Electrochim Acta, 2013, **88**: 457–462. DOI: 10.1016/j.electacta.2012.10.045

[7] Yan Y D, Tang H, Zhang M L, *et al*. Extraction of europium and electrodeposition of Al-Li-Eu alloy from Eu_2O_3 assisted by $AlCl_3$ in LiCl–KCl melt. Electrochim Acta, 2012, **59**: 531–537. DOI: 10.1016/j.electacta.2011.11.007

[8] Chen L Y, Huang M X, Gu Y L, *et al*. Low-temperature synthesis of nanocrystalline ZrP via co-reduction of $ZrCl_4$ and PCl_3. Mater Lett, 2004, **58**: 337–3339. DOI: 10.1016/j.matlet.2004.06.033

[9] Castrillejo Y, Bermejo M R, Barrado E, *et al*. Solubilization of rare earth oxides in the eutectic LiCl-KCl mixture at 450°Cand in the equimolar $CaCl_2$-NaCl melt at 550°C. J Electroanal Chem, 2003, **545**: 141–157. DOI: 10.1016/S0022-0728(03)00092-5

[10] Embarek B, Gilles M B, Jean M, *et al*. Physicochemical study of the hydrolysis of rare-earth elements (III) and thorium (IV). CR Chim, 2004, **7**: 537–545.DOI: 10.1016/j.crci.2004.01.008

[11] Sangster J and Pelton A D. The Li-W (lithium-tungsten) system. J Phase Equilib, 1991, **12**: 203–203.

[12] Wei S Q, Zhang M L, Han W, *et al*. Electrochemical codeposition of Mg-Li-Gd alloys from LiCl-KCl-$MgCl_2$-Gd_2O_3 melts. T Nonferr Metal Soc, 2011, **21**: 825–829. DOI:10.1016/S1003-6326(11)60788-7

[13] Han W, Zhang Y X, Ye K, *et al*. Electrochemical codeposition of quaternary Mg-Li-Ce-La alloys from molten salt. Metall Mater Trans B, 2010, **41**: 1123–28. DOI: 10.1007/s11663-010-9395-z

[14] Masset P, Konings R J M, Malmbeck R, *et al*. Thermochemical properties of lanthanides (Ln = La, Nd) and actinides (An = U, Np, Pu, Am) in the molten LiCl-KCl eutectic. J Nucl Mater, 2005, **344**: 173–79. DOI: 10.1016/j.jnucmat.2005.04.038